Mechanistic aspects of ammonia synthesis on Ta_3N_5 surfaces in the presence of intrinsic nitrogen vacancies

Constantinos D. Zeinalipour-Yazdi*

School of Health, Sport and Bioscience, University of East London, Stratford Campus, Water Lane, London E15 4LZ, UK

Department of Natural Sciences, Faculty of Science and Technology, Middlesex University, The Burroughs, NW4 4BT, UK

*to whom correspondence should be addressed: c.zeinalipour-yazdi@uel.ac.uk

Abstract

A possible dinitrogen activation and the ammonia synthesis mechanism was studied on the (100), (010) and (001) surface of Ta_3N_5 that contain intrinsic nitrogen vacancies. The study suggests that intrinsic nitrogen vacancies can become catalytic centers for the ammonia synthesis reaction on Ta_3N_5 via a Langmuir-Hinshelwood mechanism, which may explain the moderate production of ammonia at high temperatures. In the mechanism proposed dinitrogen is activated in a peculiar side on sandwich-like configuration between two surface Ta atoms. Calculation of the reaction activation barrier suggest that the mechanism proceeds via moderate barriers but some elementary reaction steps involve the strong adsorption of ammonia which appears to poison the surface catalytic sites on Ta_3N_5.

Keywords: ammonia synthesis mechanism; tantalum nitride; Ta_3N_5; DFT-D3

1 Introduction

It is well recognised that an important advance of chemical sciences occurs whenever the mechanism of a reaction is understood. This is particularly true for the ammonia synthesis mechanism, which has been recently the epicenter of numerous computational and experimental studies. [1-14] We have

recently become interested to understand the mechanism of ammonia synthesis reaction on various metal nitrides (i.e., Co_3Mo_3N[7], Mn_6N_{5+x}[15], η-Mn_3N_2[3]). In these studies we have attempted to address the role of promoters and defects in the ammonia synthesis reaction. It was found that there is a large number of defects (e.g. nitrogen vacancies) present at the surface of metal nitrides even at moderate temperatures. On Co_3Mo_3N surfaces these nitrogen vacancies can be of the order of 10^{13} per cm^2 even at ambient temperature. [12] It is therefore conceivable that such nitrogen vacancies could become catalytic centers for mechanistic pathways that compete with other mechanisms that occur in the absence of such vacancies. This was recently shown to occur on Co_3Mo_3N surfaces where dinitrogen was found to be considerably activated on the (111) surfaces when nitrogen vacancies where present [16] and therefore found to proceed via a novel mechanism in which nitrogen vacancies where the catalytically active sites. In this study we continue our study of interesting reaction mechanisms occurring on another metal nitride, Ta_3N_5 and in particular in the presence of nitrogen vacancies. This is the first comprehensive study of the reaction mechanism of ammonia synthesis on Ta_3N_5 done via DFT calculations. This is particularly important as there is recent evidence from Fourier transform ion cyclotron resonance mass spectrometry coupled to quantum mechanical calculations that the cleavage of the inert N-N bond can happen at room temperature on tantalum nitride clusters of the form Ta_2N^+.[17] The effect of oxygen impurities were found to stabilise Ta_3N_5 low index surfaces. [18] Nitrogen vacancies were found to result in a 720 nm sub-band-gap optical absorption.[19] The interstitial nitrogen was found to be labile and reactive to hydrogen that generates ammonia under reducing conditions.[20] We have recently experimentally screened the reactivity of ammonia synthesis on Co, Fe and Re doped Ta_3N_5 materials which has shown that Co doping results in enhanced activity[20] which is associated to the fact that cobalt dissociates H_2 efficiently.[21] In the later DFT study the adsorption of nitrogen at bridging nitrogen sites (Ta–N–Ta) results in an azide functional group formation but the molecular nitrogen adsorption is generally non-activated in defect free Ta_3N_5 surfaces. H_2 was found also to chemisorb molecularly at tantalum sites with an adsorption energy in the range −81 to −91 kJ mol^{-1}.[21] It also adsorbs

dissociatively at bridging nitrogen sites forming >NH groups.[21] Co doping especially sub-surface causes a decrease of the nitrogen vacancy formation energies on Ta_3N_5 surfaces. [21] None of the aforementioned studies indicate that ammonia synthesis may proceed on Ta_3N_5 surfaces via mechanisms that invoke nitrogen vacancies as catalytic centers. We have therefore studied this in more detail to elucidate mechanistic aspects of ammonia synthesis reaction mechanism occurring in the presence of nitrogen vacancies.

2 Computational Methods

All DFT calculations were periodic Γ-point[22] spin-polarised obtained with the use of the VASP 5.4.1 code.[23, 24] Exchange and correlation effects were considered within the generalized gradient approximation (GGA) using the revised Perdew-Burke-Ernzerhof (revPBE) exchange-correlation (XC) functional[25], with the projector augmented-wave (PAW) method[26, 27], used to represent core states. These were 1s to 5p for Ta and 1s for N, respectively. Geometry optimizations were performed with a residual force threshold on each atom of 0.02 eV $Å^{-1}$ using the conjugate-gradient algorithm. The convergence criterion for electronic relaxation was 10^{-4} eV. The planewave cutoff was set to 800 eV and the k-point convergence was achieved for the 4x4x1 Monkhorst-Pack grid which was Γ-point centered. Adsorption was only tested on one side of the slab surface as adsorbed nitrogen due to the small adsorption induced dipole expected in adsorbed di-nitrogen. Convergence of the adsorption energy of di-nitrogen was ensured with the use of a slab thickness (measured from the z-coordinate of surface nitrogen on top to surface nitrogen at the bottom of the slab) of 9.09 Å. Initial adsorption configurations where such that the distance between the adsorbate and the nearest surface site was set to 2 Å in an end-on configuration for N_2. We have used the revPBE XC functional as this was previously used to study the adsorption of N_2 and H_2 with the same surface slab with success.[21] Furthermore, comparison of this method with other methods yielded the best structural reproduction of crystallographic data for cobalt molybdenum nitride as well as prediction of the bond dissociation enthalpy of dinitrogen.[12] The initial charge density was obtained by superposition of atomic charges. The adsorption energy was taken as the total energy difference between

the fully relaxed bound state of the surface-adsorbate complex from that of the fully relaxed surface slab and the isolated molecules given by eqn. 1,

$$\Delta E_{ads,\,D3} = E_{slab\text{-}X} - E_{slab} - E_X, \quad (1)$$

where X = N_2, H_2 and N_xH_y. Grimme's dispersion corrections were included via the zero-damping DFT-D3 correction method, [28] in which the following dispersion energy correction is added to the Kohn-Sham energies,

$$E_{disp} = -\frac{1}{2}\sum_{i=1}^{N}\sum_{j=1}^{N}\left(s_6\frac{C_{6,ij}}{r_{ij}^6} + s_8\frac{C_{8,ij}}{r_{ij}^8}\right), \quad (2)$$

where $C_{6,ij}$ and $C_{8,ij}$ denote the averaged (isotropic) 6th and 8th order dispersion coefficients for atom pair ij and r_{ij} is the internuclear distance between atoms i and j, respectively. s_6 and s_8 are the functional-dependent scaling factors. The D3 correction was invoked in calculating the adsorption energies, as it is generally known that the revPBE is unable completely recover dispersion interactions as a result of polarisation effects primarily of the transition metals (TMs). Activation barriers were calculated with the nudged elastic band method as implemented in VASP. [29] Activation barriers were obtained by the nudged elastic band (NEB) method in which the barrier was modelled by 5 images.

3 Results and Discussion

The time-of-flight neutron diffraction (TOF-ND)[30] coordinates have been used to model the surface slabs of Ta_3N_5. The surface slabs that where build from a bulk 3x1x1 unit cell of Ta_3N_5 are shown in Fig. 1 and is composed of irregular TaN_6 octahedra with both three (N^3) and four coordinate nitrogen (N^4) atoms and has the pseudo-brookite (Fe_2TiO_5) structure. [31] We have formed nitrogen vacancies on the three low Miller index surfaces of Ta_3N_5 and tested how dinitrogen adsorbs to these vacancies. The starting structures for dinitrogen are shown in yellow in Fig. 1.

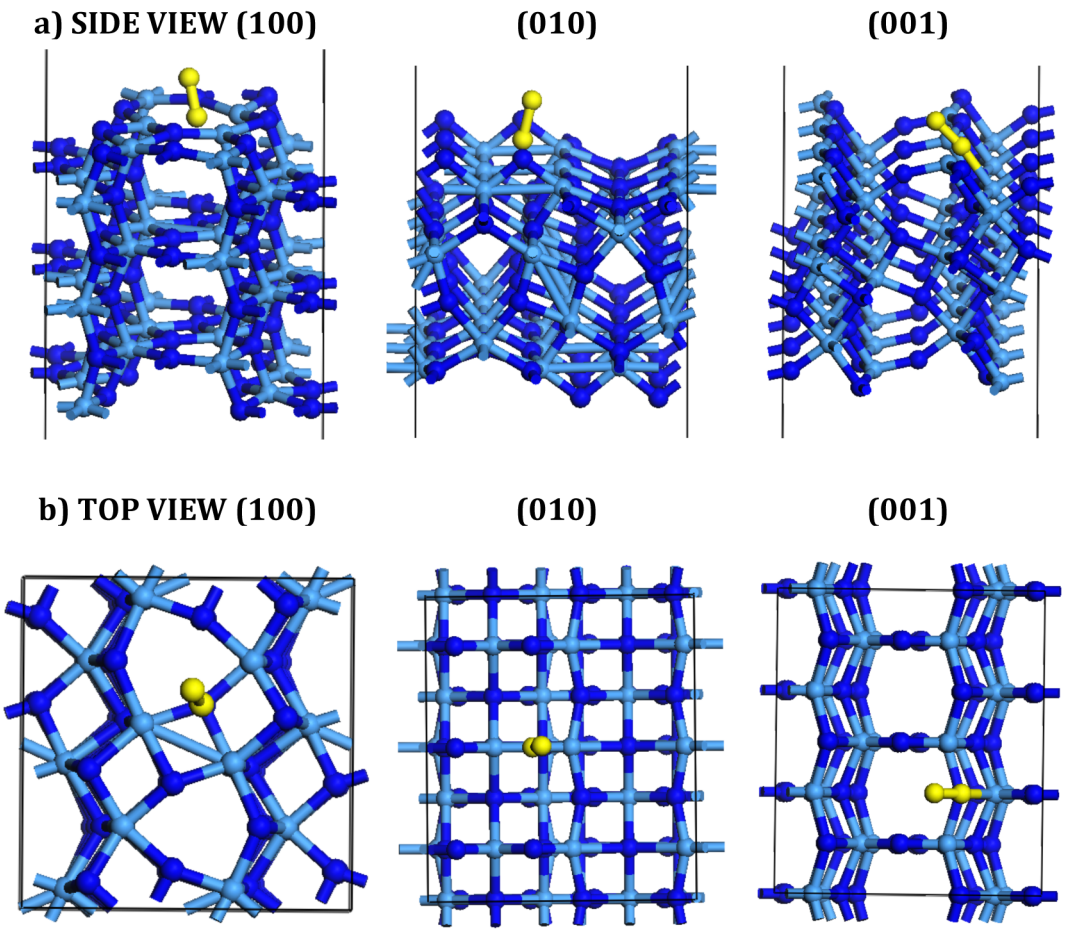

Fig. 1 (a) Side view and b) top view of Ta_3N_5 showing in yellow dinitrogen initial structure at the nitrogen vacancy of the corresponding surface (100), (010) and (001), respectively.

We have formed the various nitrogen vacancies on the three surfaces of Ta_3N_5. These nitrogen vacancies where found to be considerably higher in nitrogen vacancy formation energy than in Co_3Mo_3N.[12, 21] All three surfaces were examined with respect to their ability to activate dinitrogen and the (100)-surface was found to activate it the most based on the elongation of the N-N bond (1.367 Å). The ammonia synthesis mechanism was therefore examined on the (100) surface of Ta_3N_5.

The simplified Lewis structure mechanism of the ammonia synthesis reaction is shown in Fig. 2. It starts at **O**, which corresponds to the surface with just a nitrogen vacancy present. Nitrogen adsorbs readily in a sandwich-like configuration in which it is bound simultaneously by two tantalum atoms. This binding configuration has not been previously observed in nitrogen adsorption

studies of other metal nitrides (i.e., Co_3Mo_3N[7], Mn_6N_{5+x}[15], η-Mn_3N_2[3]). There the binding configurations of dinitrogen where primarily *end-on*, *side-on* and *tilt end-on*. It is obvious that the nitrogen vacancies on Ta_3N_5 offer a new adsorption and activation site for dinitrogen. The adsorption of N_2 at the nitrogen vacancy is slightly endothermic by 19.2 kJ mol^{-1} similar to what was previously observed for other metal nitrides (i.e., Co_3Mo_3N[7], Mn_6N_{5+x}[15], η-Mn_3N_2[3]). The adsorption of H_2 shown in **B** of Fig. 2 occurs at nearby Ta atom in a side-on configuration with a chemisorption energy of -89 kJ mol^{-1}. This is consistent with the molecular adsorption of H_2 on the defect free surface of Ta_3N_5[21], which was found to range between -82 kJ mol^{-1} to -91 kJ mol^{-1} . A second H_2 adsorbs side-on with an adsorption energy of -87 kJ mol^{-1} on an adjacent Ta atom shown in **C** of Fig. 2. In **D**, the adsorbed H_2 dissociates in order to form >N-NH< and Ta-H via a low barrier process of 50 kJ mol^{-1}. In **E**, a second hydrogenation of >N-NH< then occurs to form >N-NH_2< via another low barrier process of 57 kJ mol^{-1}. This intermediate transforms in **F** via a rather exothermic process into adsorbed ammonia and Ta-N-Ta-H. The ammonia is very strongly bound to the Ta atom and requires 231 kJ mol^{-1} to desorb as this can be seen in **G** of Fig. 2. In **H** another H_2 adsorbs molecularly to now vacant Ta atom with an adsorption energy of 88 kJ mol^{-1} consistent with the earlier values found for the chemisorption of H_2. In **I** the molecularly adsorbed H_2 dissociates to form Ta-H and N-H species via a 57 kJ mol^{-1} barrier. In **J** atomic H adsorbed to a Ta atom migrates to the adjacent >N-H forming a >NH_2 intermediate in a low barrier process of 61 kJ mol^{-1}. In **K** the >NH_2 group reacts with an adjacent hydrogen to form ammonia which is adsorbed to the Ta atom in low barrier process (65 kJ mol^{-1}). In the final step of this reaction mechanism ammonia needs to be desorbed which requires 225 kJ mol^{-1} similar to the desorption energy of ammonia found in step **G**. The mechanism modelled has distinct features that differentiate it from previously calculated reaction mechanisms found on other metal nitrides.[7] The most prominent feature is that dinitrogen becomes activated in a sandwich-like configuration, which is different than the end-on and side-on activation observed on Co_3Mo_3N containing nitrogen vacancies.[7] The other feature is that the mechanism here resembles a Langmuir-Hinshelwood mechanism where atomic hydrogen hydrogenates N_xH_y species on the surface of the catalyst. This is in

contrast with the mechanism observed on Co3Mo3N surfaces where the dominant mechanism is an Eley-Rideal / Mars van-Krevelen (E-R/MvK) mechanism.[7] The third feature is that the reaction mechanism occurs at a nitrogen vacancy which is consistent with the E-R/MvK happening on Co_3Mo_3N surfaces.[16] For the above reasons it is suggested that the mechanism found should be considered as a potential mechanistic pathway for the conversion of N_2 to NH_3 on tantalum nitride (100) surfaces.

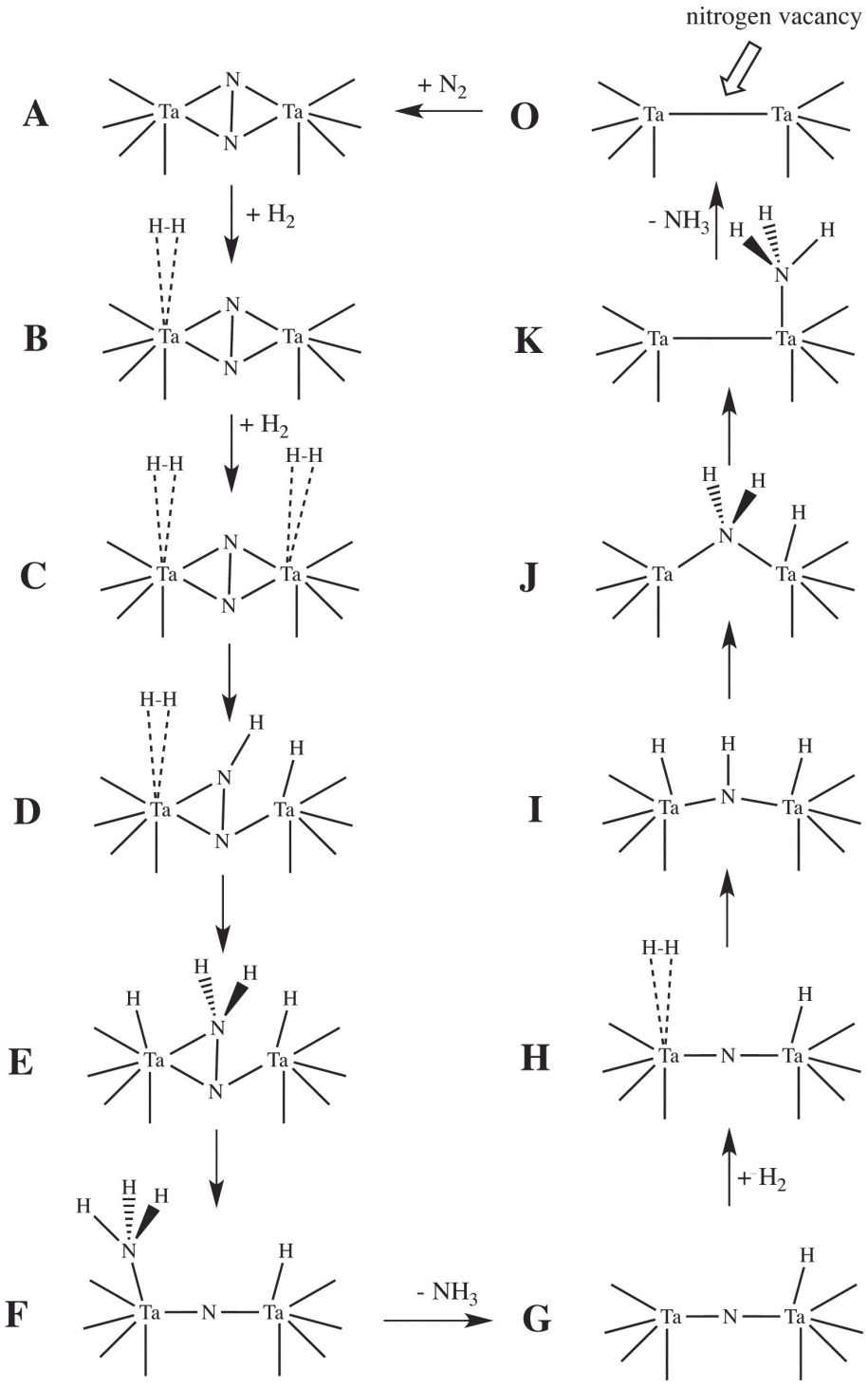

Fig. 2 Simplified Lewis structure mechanism of ammonia synthesis at nitrogen vacancies of the Ta_3N_5-(100) surface. The mechanism initiates at **O** with the adsorption of dinitrogen to a nitrogen vacancy.

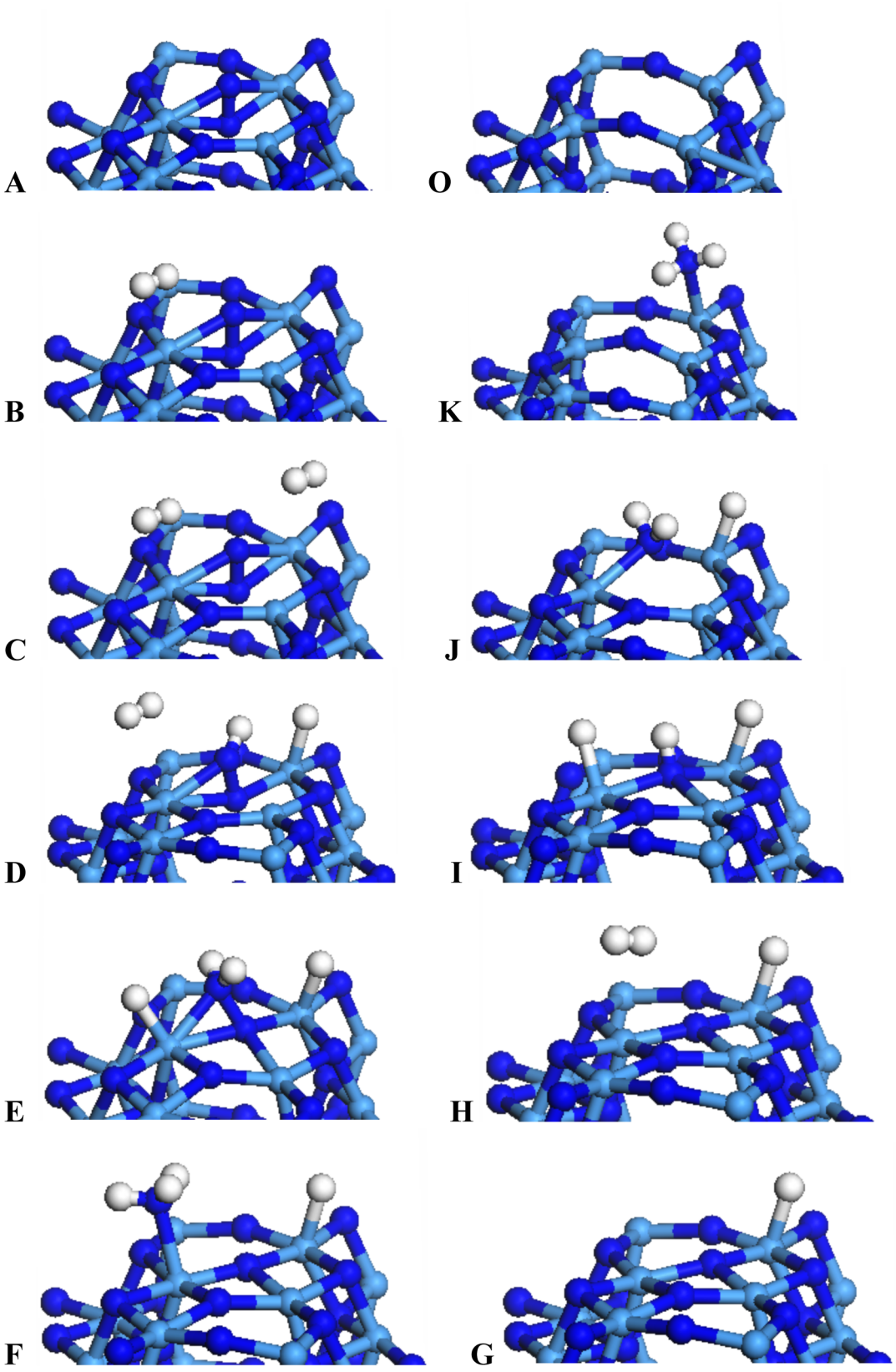

Fig. 3 Ball and stick model of the mechanism of ammonia synthesis at nitrogen vacancies of the Ta_3N_5-(100) surface. The mechanism initiates at O with the adsorption of dinitrogen to a nitrogen vacancy.

In Fig. 3 we present ball-and-stick models of the various intermediates formed on the surface of Ta_3N_5. These models offer a detailed atomistic view of the reaction mechanism for ammonia synthesis at nitrogen vacancies on Ta_3N_5-(100) surfaces.

In Fig. 4 the potential energy diagram of the reaction shows that the hydrogenation steps are relatively low barrier processes and should therefore not be prohibitive at low temperatures. However, the strong adsorption of ammonia to the catalyst could prohibit the existence of fast reaction kinetics. The product of the ammonia synthesis reaction appears to poison the catalytic sites which maybe the reason why tantalum nitride becomes active for ammonia synthesis only at high temperatures.[20] Lastly H_2, appears to adsorb stronger to the catalyst than N_2 consistent with what was found on Co_3Mo_3N[7] surfaces.

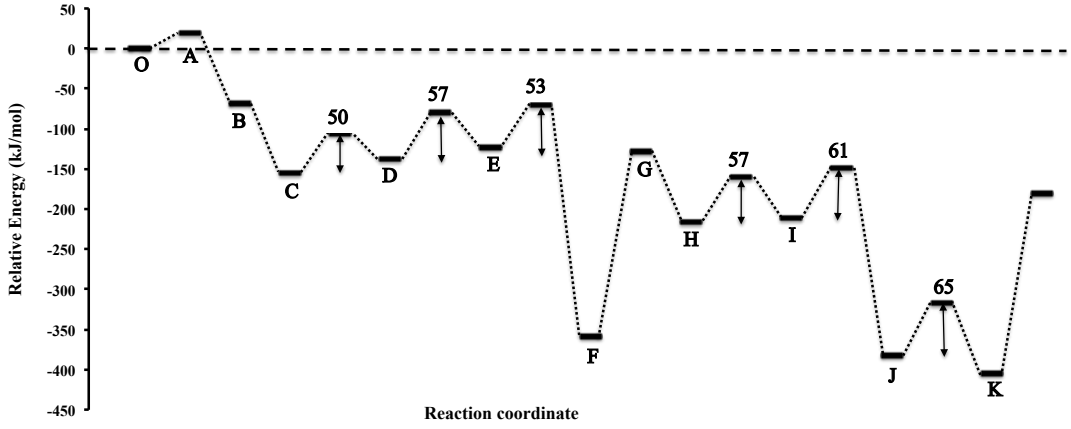

Fig. 4 Potential energy diagram of ammonia synthesis reaction mechanism on (100)-Ta_3N_5 surfaces in the presence of nitrogen vacancies.

It is suggested that for Ta_3N_5-(100) surfaces, nitrogen vacancies are necessary to perform the catalysis of the ammonia synthesis reaction. Due to the porous structure that Ta_3N_5-(100) surfaces have it is anticipated that this mechanism may also occur on other surfaces of this material.

Conclusions

Via dispersion-corrected DFT the ammonia synthesis reaction mechanism on Ta_3N_5 surfaces that have intrinsic nitrogen vacancies was studied. These atomistic DFT-D3 calculations show that there is a Langmuir-Hinshelwood

mechanism, which relies on a strong sandwich-like activation of adsorbed dinitrogen. Strong ammonia adsorption appears to be the rate-determining step for the ammonia synthesis reaction mechanism, which may explain the significant production of ammonia on Ta_3N_5 only occurs at high temperatures. This mechanistic route of ammonia synthesis on Ta_3N_5 surfaces was only found available in surfaces that contain intrinsic nitrogen vacancies.

Supporting Information

The Cartesian coordinates of the structure of the various intermediates in Figure 3 (Figure S1) are given as supporting information.

Acknowledgments

Via our membership of the UK's HEC Materials Chemistry Consortium, which is funded by EPSRC (EP/L000202/1), this work used the ARCHER UK National Supercomputing Service (http://www.archer.ac.uk).

Conflicts of Interest

The author declares no conflicts of interest.

References:

1. Y. Wang, M. Craven, X. Yu, J. Ding, P. Bryant, J. Huang and X. Tu, *ACS Catal.*, 2019, 9, 10780-10793.
2. T. Nakao, T. Tada and H. Hosono, *J. Phys. Chem. C*, 2020, 124, 2070-2078.
3. C. D. Zeinalipour-Yazdi, *Phys. Chem. Chem. Phys.*, 2019, 21, 19365-19377.
4. J. Fuller, A. Fortunelli, W. A. Goddard and Q. An, *Phys. Chem. Chem. Phys.*, 2019, 21, 11444-11454.
5. Q. An, Y. Shen, A. Fortunelli and W. A. Goddard, *J. Am. Chem. Soc.*, 2018, 140, 17702-17710.
6. J. Qian, Q. An, A. Fortunelli, R. J. Nielsen and W. A. Goddard, *J. Am. Chem. Soc.*, 2018, 140, 6288-6297.
7. C. D. Zeinalipour-Yazdi, J. S. J. Hargreaves and C. R. A. Catlow, *J. Phys. Chem. C*, 2018, 122, 6078-6082.
8. K.-i. Aika, *Catal. Today*, 2017, 286, 14-20.
9. J.-C. Liu, X.-L. Ma, Y. Li, Y.-G. Wang, H. Xiao and J. Li, *Nat. Commun.*, 2018, 9, 1610.
10. Y. Abghoui and E. Skúlason, *Catal. Today*, 2017, 286, 78-84.
11. S. Back and Y. Jung, *Phys. Chem. Chem. Phys.*, 2016, 18, 9161-9166.
12. C. D. Zeinalipour-Yazdi, J. S. J. Hargreaves. and C. R. A. Catlow, *J. Phys. Chem. C*, 2015, 119, 28368-28376.
13. A. L. Garden and E. Skúlason, *J. Phys. Chem. C*, 2015, 119, 26554-26559.

14. S. Kanbara, M. Kitano, Y. Inoue, T. Yokoyama, M. Hara and H. Hosono, *J. Am. Chem. Soc.*, 2015, 137, 14517-14524.
15. C. D. Zeinalipour-Yazdi, *Phys. Chem. Chem. Phys.*, 2018, 20, 18729-18736.
16. C. D. Zeinalipour-Yazdi, J. S. J. Hargreaves and C. R. A. Catlow, *J. Phys. Chem. C*, 2016, 120, 21390-21398.
17. C. Geng, J. Li, T. Weiske and H. Schwarz, *P. Natl. Acad. Sci. USA*, 2019, 116, 21416.
18. J. Wang, A. Ma, Z. Li, J. Jiang, J. Feng and Z. Zou, *Phys. Chem. Chem. Phys.*, 2015, 17, 23265-23272.
19. J. Wang, A. Ma, Z. Li, J. Jiang, J. Feng and Z. Zou, *Phys. Chem. Chem. Phys.*, 2015, 17, 8166-8171.
20. S. Laassiri, C. D. Zeinalipour-Yazdi, C. R. A. Catlow and J. S. J. Hargreaves, *Catal. Today*, 2017, 286, 147-154.
21. C. D. Zeinalipour-Yazdi, J. S. J. Hargreaves, S. Laassiri and C. R. A. Catlow, *Phys. Chem. Chem. Phys.*, 2017, 19, 11968-11974.
22. H. J. Monkhorst and J. D. Pack, *Phys. Rev. B*, 1976, 13, 5188.
23. G. Kresse and J. Furthmüller, *Phys. Rev. B*, 1996, 54, 11169–11186.
24. G. Kresse and J. Hafner, *Phys. Rev. B*, 1993, 47, 558.
25. J. P. Perdew, K. Burke and M. Ernzerhof, *Phys. Rev. Lett.* , 1996, 77, 3865.
26. P. E. Blöchl, *Phys. Rev. B*, 1994, 50, 17953.
27. G. Kresse and D. Jouber, *Phys. Rev. B*, 1999, 59, 1758–1775.
28. S. Grimme, J. Antony, S. Ehrlich and H. Krieg, *J. Chem. Phys.*, 2010, 132, 154104.
29. G. Mills, H. Jónsson and G. K. Schenter, *Surf. Sci.*, 1995, 324, 305-337.
30. N. E. Brese, M. O'Keeffe, P. Rauch and F. J. DiSalvo, *Acta Crystallogr., Sect. C: Cryst. Struct. Commun.*, 1991, 47, 2291-2294.
31. S. J. Henderson and A. L. Hector, *J. Solid State Chem.*, 2006, 179, 3518-3524.